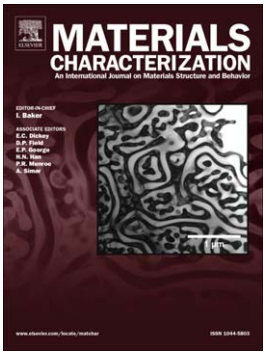

Deformation Mechanism and Microstructure Evolution During On-Line Heating Rolling of AZ31B Mg Thin Sheets

Fusheng Pan, Bin Zeng, Bin Jiang, Andrejs Atrens, Hanwu Dong

PII: S1044-5803(17)30067-0
DOI: doi:10.1016/j.matchar.2017.01.007
Reference: MTL 8519

To appear in: *Materials Characterization*

Received date: 16 September 2016
Revised date: 13 December 2016
Accepted date: 8 January 2017

Please cite this article as: Pan Fusheng, Zeng Bin, Jiang Bin, Atrens Andrejs, Dong Hanwu, Deformation Mechanism and Microstructure Evolution During On-Line Heating Rolling of AZ31B Mg Thin Sheets, *Materials Characterization* (2017), doi:10.1016/j.matchar.2017.01.007

Deformation Mechanism and Microstructure Evolution During On-Line Heating Rolling of AZ31B Mg Thin Sheets

Fusheng PAN[1,2,3,*]; Bin ZENG[1,2,*]; Bin JIANG[1,2,3]; Andrejs ATRENS[4]; Hanwu DONG[2];

1. College of Materials Science and Engineering, Chongqing University, Chongqing 400044, China

2. Chongqing Academy of Science and Technology, Chongqing 401123, China

3. National Engineering Research Center for Magnesium Alloys, Chongqing University, Chongqing 400044, China

4. School of Mechanical and Mining Engineering, The University of Queensland, St Lucia, QLD 4072, Australia

*Corresponding authors

Phone number:+86-023-67300705;

Fax number:+86-023-67300592;

E-mail addresses: fspan@cqu.edu.cn (F. Pan);zengbincastmg@163.com(B.Zeng)

Abstract: An AZ31B sheets were processed by on-line heating rolling (ON-LHR) in five passes. Roll and sheets temperatures were 473 K and 533 K, respectively. The grain size was reduced in the first three roll passes, to a minimum of 4.1 μm, due to dynamic recrystallization, and coarsened in the last two passes due to a combination of dynamic recrystallization and grain growth. The yield strength, ultimate tensile strength and elongation to fracture reached 232 MPa, 347 MPa and 21% in the rolling direction. The maximum yield strength occurred after the fourth pass. The maximum is attributed to the small grain size and the formation of networks of sub-grains and deformed grains. The rolled sheets had a strong basal texture, which was largely unchanged with the number of roll passes. The existence of the strong texture after rolling indicated discontinuous dynamic recrystallization.

Key Words: Magnesium alloys; rolling; on-line heating; EBSD; dynamic recrystallizaton

1 INTRODUCTION

Magnesium alloys are important structural metals, due to their low density, high specific strength and stiffness, and good shock absorption ability [1,2]. These good properties have allowed automobile manufactures to replace traditional materials with magnesium alloys, in order to reduce the weight of automobile components [3].

Stamping can be used to produce many auto components, but their potential current costs are too large. The current high cost of magnesium alloy sheet occurs because of the low production efficiency of rolling magnesium alloys, caused by the small possible reduction in thickness per pass [4]. The poor formability of magnesium alloys is closely associated with their hexagonal close-packed lattice structure, which limits the number of active slip systems [5–7]. This current research work is part of the extensive effort exploring the significant reduction of the cost of producing magnesium alloy sheet.

Much effort to improve the formability of Mg alloys has been devoted to (i) finding suitable deformation conditions, such as temperature and pass reduction, and (ii) the relationship with resulting mechanical properties. The grain size can be refined steadily with rolling passes due to dynamic recrystallization (DRX) [8], and the enhanced uniform elongation had been strongly correlated with improved strain-hardening due to solid solution strengthening and/or the fine precipitates in Mg alloys [9]. Moreover, the processing conditions are important. At a low rolling speed, increasing thickness reduction caused a reduction in the magnesium alloy strength and ductility, due to twinning; whereas at a high rolling speed, increasing thickness

reduction caused significant grain refinement due to dynamic recrystallization. Both strength and ductility were improved by dynamic recrystallization [10].

The dynamic recrystallization mechanisms are discontinuous dynamic recrystallization (DDRX), continuous dynamic recrystallization (CDRX), twinning induced dynamic recrystallization (TDRX) and particle-stimulated nucleation (PSN) [11]. Recrystallization is the formation of new grains with high angle grain boundaries (HAGBs) in a deformed material [12]. In discontinuous dynamic recrystallization (DDRX), the new grains are formed by the nucleation and the growth of new, stain-free, fine, randomly-oriented, grains during deformation at an elevated temperature. The new strain-free grains restore ductility [13]. In discontinuous dynamic recrystallization, the new, recrystallized grains are typically nucleated at existing grain boundaries and the new grains are fine and equiaxed [12]. In contrast, continuous dynamic recrystallization (CDRX) occurs when sub-grains are formed with low angle grain boundaries (LAGBs) during hot deformation, and these sub-grains turn into gains with high angle grain boundaries (HAGBs) with increasing deformation. Thus, the low angle grain boundaries transform into high angle grain boundaries by a progressive increase of the mis-orientation [12]. As a result, large strains produce a strong crystallographic texture [12]. The key difference between these two mechanisms of dynamic recrystallization is that discontinuous dynamic recrystallization is discontinuous, whereas continuous dynamic recrystallization is continuous [12]. TDRX results in the nucleation of grains of new orientations [14]. New grains are formed with c-axis orientations almost identical to that of the twin

host, and have a random rotation of basal planes. The PSN mechanism provides more randomly oriented nuclei, which gives rise to weaker recrystallization textures [15].

Grain size is important in determining strength as is indicated by the Hall-Petch relationship [16–20]. For magnesium alloy sheets, finer grains have been achieved by severe plastic deformation. However, the mechanical properties are also influenced by other factors such as the type of grain (i.e. deformed grains and sub-grains), grain shape and grain distribution. In addition, the evolution of microstructure in magnesium alloy thin sheets is of special importance for the mechanical properties.

Our previous work [21] developed a new rolling technique designated "on-line-heating rolling" (ON-LHR), in which the temperature of Mg alloy sheet is controlled on-line by electric-resistance heating during rolling. This means that the Mg alloy temperature can be accurately controlled, and the Mg alloy temperature can be different to the temperature of the rolls. Furthermore, with on-line heating there is no need for a reheating furnace to reheat (or anneal) the Mg alloy after each pass.

The prior art can be described as off-line-heating rolling (OFF-LHR), in which there is a need for a furnace to anneal the Mg alloy after each pass. During ON-LHR, the sheet is heated to the required temperature by electric-resistance heating during rolling. This procedure has less heat loss, because there can be significant heat loss during OFF-LHR during the time the Mg sheet is moved from the holding furnace to the rolling process. Furthermore, there is much better temperature control during ON-LHR, because the temperature is controlled directly.

The present work continues the investigation of on-line-heating rolling. The

present work studied the influence of the number of roll passes on the deformation mechanism, microstructure and mechanical properties for a thin AZ31B magnesium alloy processed by on-line-heating rolling.

2.EXPERIMENTAL PROCEDURES

The starting material was AZ31B (Mg-2.98wt.%Al-0.87wt.%Zn-0.35wt.%Mn) Mg alloy sheet with dimensions of 600 mm × 100 mm × 4 mm (length, width and thickness) as in our previous research [21]. Fig. 1 provides a schematic of the on-line-heating rolling. The rolling was performed using a four-high rolling mill with the support rolls and work rolls of 320 mm and 120 mm diameter, respectively. During rolling, there was no reheating between passes. For each pass, the thickness reduction was 25~30%. The roll and sheet temperatures were controlled to be 473 K and 533 K, respectively. A final sheet thickness of about 0.8 mm, with a total cumulative reduction of about 80%, was achieved in five passes. The rolling was carried out such that there were available for mechanical property evaluation after each roll pass at least five rolled specimens, which had thicknesses of 2.9, 2.2, 1.6, 1.1, 0.8 mm.

Dog-bone tensile specimens, with a 8 mm gauge width and a 30 mm gauge length, were prepared from these sheets with different rolling reductions, at angles of 0° (rolling direction, RD) and 90° (transverse direction, TD) to the rolling direction. Tensile tests were conducted at room temperature using an initial strain rate of 5.6×10^{-4} s^{-1} on a universal testing machine. For each condition, three tensile specimens

were tested. The yield strength was measured at a permanent elongation of 0.2%.

The electron back-scatter diffraction (EBSD) technique was used to characterize the microstructure and texture of the rolled samples. Orientation patterns were collected using a field-emission gun scanning electron microscope (FEI Nova SEM 450). The mapping was carried out for an investigated area of 150 μm × 100 μm and a step size of 0.7 μm, using the data acquisition software program HKL Channel 5. The sample surface was ground, polished, electro-polished, rinsed with methanol and dried with filter paper.

The macro-texture measurements were carried on the surface of the sheet (RD-TD plane) prepared by mechanical grinding. The {0002} and $\{10\bar{1}0\}$ pole figures of the rolled Mg alloys were investigated using X-ray diffraction (using Rigaku D/Max 2500 PC).

The different types of grains were determined based on grain orientation determined using the EBSD technique from their Kikuchi patterns. The following steps were followed by the software package "Tango" during the evaluation of deformed, sub-grain and recrystallized fractions:

I. First Tango does a grain reconstruction (using user defined parameters in the grain area determination window).
II. Then, for each grain, the internal average misorientation angle within the grain is measured.
III. If the average angle in a grain exceeds the user-defined minimum angle to define a sub-grain, ($\theta_c = 5^0$), and there is a narrow spread of measured angles, then the

grain is classified as being "deformed".

IV, Some grains consist of sub-grains whose internal mis-orientations is under θ_c but the misorientation from sub-grains to sub-grains is above θ_c. In that case the grain is classed as "sub-structured", and consists of sub-grains.

V. All the remaining grains are classified as recrystallized.

3 RESULTS AND DISCUSSION

3.1 Mechanical properties

Fig. 2 presents the stress-strain curves of the AZ31B Mg alloy at room temperature and with an initial strain rate of 5.6×10^{-4} s^{-1} after different rolling passes, and Fig. 3 presents the resulting mechanical properties. Fig. 2 and 3 show that, with increasing number of the roll passes, the yield strength (YS) and ultimate tensile strength (UTS) increased for passes 1-4 and decreased somewhat for pass 5, whereas, the elongation to fracture (FE) had a maximum value after pass 2 and a minimum value after pass 5. All the YS values were somewhat higher in the transverse direction (TD) than in the rolling direction (RD).

Both the mechanical strength and the elongation to fracture of the AZ31B Mg alloy were relatively high. The yield strength (YS), ultimate tensile strength (UTS) and elongation to fracture of the original alloy were 210~220 MPa, 330 MPa and 16~17%, respectively. In comparison, after four roll passes, the YS, UTS and elongation to fracture of the AZ31B were 260~270 MPa, 350 MPa and 16~18%, respectively, indicating that the mechanical properties were improved by

on-line-heating rolling. The best combination of properties was after pass 3. The YS, UTS and ductility were 232 MPa, 347 MPa, 21% in the rolling direction, and 242 MPa, 341 MPa, 18% in the transverse direction.

Fig. 2 indicates that all the stress-strain curves, except the fifth roll pass curve, had a power-law type work hardening region. The starting material showed almost continuous work hardening until fracture of the tensile specimen. For the as-rolled sheets, the power law type work hardening region in the stress-strain curves was similar and followed by a similarly-short post-UTS region. Moreover, the insert in Fig. 2 shows that the material after pass 5 had an obvious yielding step, and the YS and UTS were a little lower than after the fourth pass. The total rolling reduction was increased from 70% to 80% with actual thickness reduced from 1.1 mm to 0.8 mm.

The strain-hardening exponent (n) is a measure of metal plasticity, with increasing values providing increasing amounts of uniform plastic strain, so that the material can be stretched further before necking starts [22]. The strain hardening behavior of the initial and as-rolled samples were analyzed assuming that the stress-strain curve could be expressed by the famous Ludwik-Hollomon relation as follows:

$$\sigma = K_1 + K_2\varepsilon^n \qquad (1)$$

where σ and ε are the true stress and strain, respectively, n is the strain hardening exponent, and K_1 and K_2 are the strength coefficients. The differentiation of the logarithmic form of equation (1) with respect to ε, gives:

$$\mathrm{Ln}\sigma = \mathrm{Ln}K_1 + n\mathrm{Ln}K_2\varepsilon \qquad (2)$$

The n values calculated from the slope of the ln σ versus ln ε curve are presented in Fig. 3. The n values of the initial sample were 0.18 and 0.17 in the rolling direction and transverse direction, respectively. The n values decreased with increasing number of roll passes. This can be attributed to the high dislocation density after each roll pass, which hindered the subsequent dislocation storage during tensile deformation, consistent with Kaseem et al. [23]. The n values in the rolling direction were always somewhat higher than those in the transverse direction.

The advantages of ON-LHR compared with OFF-LHR (off-line heating rolling) is that (i) there does not need to be an annealing treatment in the holding furnace after each pass, and that (ii) the temperature control of the sheets are better during ON-LHR. Table 1 provides comparison mechanical properties of AZ31B processed by OFF-LHR, in which the sheets were processed by rolling with interpass reheating in multiple passes with or without annealing treatments. This present study shows that both the strength and the ductility of AZ31B Mg alloy sheet can be improved by ON-LHR without any additional treatments.

3.2 Microstructure evolution

Fig. 4 and Fig. 5 show the inverse pole figures (IPFs) and the frequency-misorientation maps for AZ31B, for both the starting material, and the as-rolled after various roll passes. All these six IPFs look visually red with only a few spots of green color and/or blue color interspersed. The different colors represent grains with different orientations. The fan-shaped icon in Fig. 4(g) indicates that the

majority of grains were orientated with their c-axis along the normal direction (ND). The nearly identical colored grains mean that the mis-orientations between these grains were not large. Table 2 indicates that the frequency of low angle grain boundaries (LAGBs) ($\leqslant 15^{o}$) of the original material was high, about 70%, which could also explain the strong texture of the AZ31B alloy. Fig. 5 indicates that there were a large number of grains with a small degree of mis-orientation, indicative of sub-grains.

These IPFs and the frequency-misorientation maps allow identification of the dynamic recrystallization mechanism as continuous dynamic recrystallization (CDRX) because of (i) the formation of low-angle boundaries within the grains, and (ii) the formation of a strong texture after rolling. Continuous dynamic recrystallization is expected to produce low angle boundaries and a strong texture [12].

For hot working with dynamic recrystallization, the grain size is dependent on the deformation temperature, the deformation amount, and the strain rate [8]. Fig. 6 presents the grain size distribution for the AZ31B prior to rolling and after rolling. Fig. 6, combined with Fig. 4, indicates that the grains were refined after rolling. For all the samples, the grain size distributions displayed a single peak. The starting material consisted of relatively-coarse, equiaxed grains, 14.0 μm in average size, with no evidence of twinning. After the first roll pass (Fig. 4(b)), there was a dynamically recrystallized (DRXed) microstructure, with a medium grain size of 6.9 μm. Dynamic recrystallization during the first roll pass at 533 K helped to refine the AZ31B microstructure, but full recrystallization was not achieved, due possibly to the starting

coarse microstructure. After the second roll pass (Fig. 4(c)), there was a similar but finer dynamically recrystallized microstructure, with the largest size of the coarse grains decreased to 12 μm. After the third roll pass with a total thickness reduction of 60%, there was a homogeneous dynamically recrystallized microstructure with equiaxed grains of about 4.1 μm in average size, as illustrated in Fig. 4(d). The range of grain size after the third roll pass was the narrowest for all the specimens. The results shown in Fig. 4 (a-d) indicate that the grains were refined and the microstructure homogeneity improved steadily by dynamic recrystallization with a relatively low rolling temperature (533 K) through repeated hot rolling with thickness reductions of 25~30% per pass. Similar results were also reported in Refs. [24–26].

Fig. 6(e) indicates that there was a slight increase in the average grain size after the fourth roll pass, which can be attributed to the increase in the span of the grain size spectrum, and Fig. 6(f) indicates that the grain size of the fifth pass slightly rose to 5.5 μm.

3.3 Texture analysis

Fig. 7 shows the {0002} and $\{10\bar{1}0\}$ pole figures for AZ31B sheets rolled after different roll passes. The major texture components of all the specimens could be expressed as ND // {0001} basal texture. The as-rolled sheets exhibited a strong basal texture. The maximum pole intensity of the {0002} pole figure for the original sheet was 22.0. The maximum pole intensity of the {0002} pole figures changed to 13.6, 14.0, 14.8, 16.1 and 15.1 after the first to fifth roll pass, respectively, indicating a

somewhat smaller maximum pole intensity compared with the original sheet, with a narrow range of 13.6 to 16.1. The maximum pole intensity of the {0002} pole figure had the same trend with the YS of the rolled sheets from first to fifth pass.

Fig.7(b) to fig.7(f) indicate that the texture type and intensity had little change indicating that the number of roll passes had only a small impact on the macro-texture of the sheet, under the condition of this experiment. This confirms that the mechanism of dynamic recrystallization in this study was not discontinuous dynamic recrystallization (DDRX) because DDRX forms new grains with mis-orientations of 5-20° to that of the adjacent parent grains [27,28]. The no significant change in crystallographic texture is consistent with expectations from continuous dynamic recrystallization (CDRX) [7,26].

3.4 Deformation mechanism

Grain boundaries play two complementary roles in polycrystals. On the one hand, the grain boundary is an obstacle to dislocation motion. On the other hand, the deformation coordination requirements mean that a different slip system may become operational in the different grain. The coordination of five separate slip system is needed, independent of grain size. The plasticity resistance is related to grain size, with decreasing grain size increasing the resistance to plastic flow, which indicates that the grain boundaries are playing a role of reinforcement.

The average grain size of the as-rolled sheets were 6.9 μm, 5.7 μm, 4.1 μm, 4.5 μm and 5.5 μm respectively, corresponding to the first to the fifth pass. These were all

much finer than that of the starting material of 14.0 μm. The YS as a function of grain size can be expressed as Hall-Petch relationship:

$$\sigma_s = \sigma_0 + kd^{-0.5} \quad (3)$$

where d is the average grain diameter, σ_0 is the YS of a single crystal, and k is a constant for a specific material. In the present study, Fig. 3 shows that the YS increased with the number of roll passes for the first four passes, which was related to the decrease in grain size for the first three passes as expected from the Hall-Petch relationship.

However, the grain size after the fourth roll pass was 4.5 μm, somewhat larger than after the third roll pass, 4.1 μm, so the increase in yield strength after the fourth pass was at first glance contrary to the expectation from the Hall-Petch relation. However the reason could be related to the distribution of different grain areas.

Fig. 8 presents the recrystallization maps as determined by EBSD after the different roll passes, with the recrystallized grains, subgrains and deformed grains colored blue, yellow and red, respectively. The different types of grains were determined based on grain orientation determined from their Kikuchi patterns. The definition of recrystallized structure here is based on the magnitude of mis-orientation angle over a local region, which could be used as a criterion for the evaluation of structural recovery during plastic deformation. From Fig. 8(a) to 8(c), with the small decrease in grain size, from 6.9 μm to 4.1 μm, the fraction of recrystallized grains increased from 65% to 75%. From Fig. 8 (c) to 8(e), the condition was reversed, although the grain size grew from 4.1 μm to 5.5 μm, the fraction of recrystallized grains decreased greatly from 75% to 35%, whereas the fraction of subgrains increased from 14% to 47%. Because of their difference in dislocation density, the

three types of grains have increasing strength, in the sequence from recrystallized grains, sub-grains and deformed grains. The YS increases with the area increase of the latter two grain types under the premise that these grains can connect with each other to form framework structures. Fig. 8 (a) to 8(c) indicate that there was not any network formed by the sub-grains and deformed grains, and for this condition, the YS was determined only by the decreasing recrystallized grain size. In Fig. 8 (d) and (e), throughout the whole images, the sub-grains and the deformed grains are connected like a net by sharing their boundaries, and formed frameworks. This is the reason that for the relatively high YS values in these cases.

Fig. 8, combined with Fig. 5, indicated that after the first pass to the third roll pass, fine recrystallization grains formed, and the orientation of these grains was similar, which reduced the proportion of the low angle grain boundaries (LAGBs). Fig. 8(c) indicates a large number of fine uniform recrystallized grains, about 2 μm, which almost entirely surround the retained large grains. This is the reason that ductility after the third roll pass was the optimum, and the YS was higher than after the former two passes. However, Fig. 8 (d) and (e) show that there were no small recrystallized grains after the fourth and fifth passes, but the recrystallized grains grew in size, and these grains had a strong orientation, as presented in Table 2.

If there is sufficient dynamic recrystallization during hot rolling, the sheets remain formable and then the sheets can be continuously rolled thinner and thinner. However, in the present study, as well in the literature [9,29–31], the results show that, irrespective of the parameters such as pass reduction and rolling rate, there is edge cracking when the rolling has proceeded beyond a certain number of passes.

In the present study, where the rolling was conducted at 533 K, small edge cracks were formed during the fourth pass and then larger edge cracks in the fifth pass, which are the forerunners of sheet fracture through experience. That is to say, the sheets have reached the limit of formability after five roll passes.

The expectation based on dynamic recovery is thus different to the actual experimental experience. However, of all the factors that may affect the formability of the sheets, the thickness is the one that changed the most. With decreasing sheet thickness, there was a decrease in the average grain size and grain size distribution, and also a change in the fraction of various types of grains, which as comprehensive factors affect the mechanical properties of the material.

4 CONCLUSION

The present work studied the influence of the number of roll passes on the deformation mechanism, microstructure and mechanical properties for a thin AZ31B magnesium alloy processed by on-line-heating rolling.

(1) The grain size decreased with the increasing rolling passes for the first three roll passes due to dynamic recrystallization. The average grain sizes were 6.9 μm, 5.7 μm and 4.1 μm, respectively. The grain size increased after the fourth pass and the fifth passes. The average grain sizes were 4.5 μm and 5.5 μm respectively.

(2) The third pass created the best overall mechanical properties with the YS, UTS and elongation to fracture (FE) reaching 232 MPa, 347 MPa and 21%

respectively in the rolling direction and 242 MPa, 341 MPa and 18.% respectively in the traverse direction.

(3) The yield strength of the AZ31B thin sheets increased after the first three roll passes due to decreasing grain size. The maximum yield strength occurred after the fourth roll pass because the strengthening due to the sub-grain networks overcame the effect of a slightly larger grain size.

(4) The texture type and intensity had little change indicating that the number of roll passes had only a small impact on the macrotexture of the sheet, under the condition of this experiment.

(5) The existence of the strong texture after rolling indicated discontinuous dynamic recrystallization.

ACKNOWLEDGEMENTS

This work was financially supported by the International Science and Technology Cooperation Project (2014DFG52810), National Natural Science Foundation of China (Grant NO.51504052), and the foundations from Chongqing Science and Technology Commission (CSTC2013JCYJC60001).

REFERANCE

[1] L. Lu, T. Liu, Y. Chen, Z. Wang, Deformation and fracture behavior of hot extruded Mg alloys AZ31, Mater. Charact. 67 (2012) 93–100.

[2] J.P. Young, H. Askari, Y. Hovanski, M.J. Heiden, D.P. Field, Thermal microstructural stability of AZ31 magnesium after severe plastic deformation, Mater. Charact. 101 (2015) 9–19.

[3] B.L. Mordike, T. Ebert, Magnesium Properties — applications — potential, Mater. Sci. Eng. A. 302 (2001) 37–45.

[4] D. Liu, Z. Liu, E. Wang, Effect of rolling reduction on microstructure, texture,

mechanical properties and mechanical anisotropy of AZ31 magnesium alloys, Mater. Sci. Eng. A. 612 (2014) 208–213.

[5] Y. Chen, L. Jin, J. Dong, Z. Zhang, F. Wang, Twinning effects on the hot deformation behavior of AZ31 Mg alloy, Mater. Charact. 118 (2016) 363–369.

[6] J. Sun, L. Jin, J. Dong, W. Ding, A.A. Luo, Microscopic deformation compatibility during monotonic loading in a Mg-Gd-Y alloy, Mater. Charact. 119 (2016) 195–199.

[7] J. Su, M. Sanjari, A.S.H. Kabir, I. Jung, S. Yue, Dynamic recrystallization mechanisms during high speed rolling of Mg – 3Al – 1Zn alloy sheets, Scr. Mater. 113 (2016) 198–201.

[8] M. Qing, H.U. Lian-xi, S.U.N. Hong-fei, W. Er-de, Grain refining and property improvement of AZ31 Mg alloy by hot rolling, Trans. Nonferrous Met. Soc. China. 19 (2009) s326–s330.

[9] W. Chen, W. Zhang, Y. Qiao, Q. Miao, E. Wang, Enhanced ductility in high-strength fine-grained magnesium and magnesium alloy sheets processed via multi-pass rolling with lowered temperature, J. Alloys Compd. 665 (2016) 13–20.

[10] F. Guo, D. Zhang, X. Yang, L. Jiang, S. Chai, F. Pan, Materials Science & Engineering A Effect of rolling speed on microstructure and mechanical properties of AZ31 Mg alloys rolled with a wide thickness reduction range, Mater. Sci. Eng. A. 619 (2014) 66–72.

[11] J. Zhang, B. Chen, C. Liu, Materials Science & Engineering A An investigation of dynamic recrystallization behavior of ZK60-Er magnesium alloy, Mater. Sci. Eng. A. 612 (2014) 253–266.

[12] K. Huang, R.E. Logé, A review of dynamic recrystallization phenomena in metallic materials, JMADE. 111 (2016) 548–574.

[13] F. Berge, Influence of temperature and strain rate on flow stress behavior of twin-roll cast, rolled and heat-treated AZ31 magnesium alloys, Trans. Nonferrous Met. Soc. China (English Ed. 25 (2015) 1–13.

[14] S. Yi, I. Schestakow, S. Zaefferer, Twinning-related microstructural evolution during hot rolling and subsequent annealing of pure magnesium, 516 (2009) 58–64.

[15] J.D. Robson, D.T. Henry, B. Davis, Particle effects on recrystallization in magnesium – manganese alloys□: Particle-stimulated nucleation, Acta Mater. 57 (2009) 2739–2747.

[16] S. Liang, H. Sun, Z. Liu, E. Wang, Mechanical properties and texture evolution during rolling process of an AZ31 Mg alloy, J. Alloys Compd. 472 (2009) 127–132.

[17] T. Zhou, Z. Yang, D. Hu, T. Feng, M. Yang, X. Zhai, Effect of the final rolling speeds on the stretch formability of AZ31 alloy sheet rolled at a high temperature, J. Alloys Compd. 650 (2015) 436–443.

[18] F. Guo, D. Zhang, X. Yang, L. Jiang, S. Chai, F. Pan, Influence of rolling speed on microstructure and mechanical properties of AZ31 Mg alloy rolled by large strain hot rolling, Mater. Sci. Eng. A. 607 (2014) 383–389.

[19] K. Hamad, B.K. Chung, Y.G. Ko, Microstructure and mechanical properties of severely deformed Mg-3%Al-1%Zn alloy via isothermal differential speed rolling at 453 K, J. Alloys Compd. 615 (2015) S590–S594.
[20] W.J. Kim, S.W. Chung, Superplasticity in Fine-grained AZ61 Magnesium Alloy, Met. Mater. Int. 3 (2000) 255–259.
[21] F. Pan, B. Zeng, B. Jiang, M. Zhang, H. Dong, Enhanced mechanical properties of AZ31B magnesium alloy thin sheets processed by on-line heating rolling, 693 (2017) 414–420.
[22] P. Movahed, S. Kolahgar, S.P.H. Marashi, M. Pouranvari, N. Parvin, The effect of intercritical heat treatment temperature on the tensile properties and work hardening behavior of ferrite – martensite dual phase steel sheets, Mater. Sci. Eng. A. 518 (2009) 1–6.
[23] M. Kaseem, B.K. Chung, H.W. Yang, K. Hamad, Y.G. Ko, Journal of Materials Science & Technology Effect of Deformation Temperature on Microstructure and Mechanical Properties of AZ31 Mg Alloy Processed by Differential-Speed Rolling, J. Mater. Sci. Technol. 31 (2015) 498–503.
[24] Q. Miao, L. Hu, G. Wang, E. Wang, Fabrication of excellent mechanical properties AZ31 magnesium alloy sheets by conventional rolling and subsequent annealing, Mater. Sci. Eng. A. 528 (2011) 6694–6701.
[25] T.C. Chang, J.Y. Wang, C.M. O, S. Lee, Grain refining of magnesium alloy AZ31 by rolling, J. Mater. Process. Technol. 140 (2003) 588–591.
[26] J.A. Valle, J.M. Contreras, O.A. Ruano, Microstructural evolution during large strain hot rolling of an AM60 Mg alloy, 50 (2004) 661–665.
[27] D. Ponge, G. Gottstein, Necklace Formation During Dynamic Recrystallization:Mechanisms and Impact on Flow Behavior, 46 (1998) 69–80.
[28] M.R. Barnett, A. Sullivan, N. Stanford, N. Ross, A. Beer, Texture selection mechanisms in uniaxially extruded magnesium alloys, Scr. Mater. 63 (2010) 721–724.
[29] S. Kim, D. Kim, Y. Lee, C. Oh, K. Lee, H.N. Han, Influence of Constraint Condition on Rolling Behavior of Magnesium Alloy at Low Temperatures, Met. Mater. Int. 21 (2015) 719–725.
[30] C.D. Yim, Y.M. Seo, B.S. You, Effect of the Reduction Ratio per Pass on the Microstructure of a Hot-Rolled AZ31 Magnesium Alloy Sheet, Met. Mater. Int. 15 (2009) 683–688..
[31] Y. Ding, Q. Le, Z. Zhang, L. Bao, J. Cao, J. Cui, Effect of vertical rolling at various temperatures on subsequent multi-pass severe rolling of AZ31B alloy sheet, J. Mater. Process. Technol. 213 (2013) 2101–2108.
[32] Q. Zhang, Effect of rolling method on microstructure and properties of AZ31 magnesium alloy thin sheet, Chinese J. Nonferrous Met. 14 (2004) 391–397.
[33] Lingyun Wang, Research on Rolling Technology of Magnesium Alloy Sheets, Rare Met. Mater. Eng. 36 (2007) 910–914.
[34] H. Zhang, W. Cheng, J. Fan, B. Xu, H. Dong, Improved mechanical properties of AZ31 magnesium alloy sheets by repeated cold rolling and annealing using a small pass reduction, Mater. Sci. Eng. A. 637 (2015) 243–250.

[35] H. Watanabe, T. Mukai, K. Ishikawa, Effect of temperature of differential speed rolling on room temperature mechanical properties and texture in an AZ31 magnesium alloy, J. Mater. Process. Technol. 182 (2007) 644–647.

[36] X. Huang, K. Suzuki, N. Saito, Enhancement of stretch formability of Mg-3Al-1Zn alloy sheet using hot rolling at high temperatures up to 823 K and subsequent warm rolling, Scr. Mater. 61 (2009) 445–448.

Table 1. Representative mechanical properties of AZ31 magnesium alloy sheets at room temperature processed using off-line-heating rolling.

Temp. (K)	Thickness(mm)	Average UTS(MPa)			Average YS(MPa)			Average FE(%)			Ref.
		RD	DD	TD	RD	DD	TD	RD	DD	TD	
623-673K	0.5	320	—	383	250	—	310	6	—	7.4	[32]
573K	2	228	230	233	—	—	—	17.5	18.5	18	[33]
< 533K	1.6	288	285	286	—	—	—	15	16	17	
673K	1	286	—	317	242	—	276	3.8	—	12.2	[25]
	0.5	301	—	325	253	—	273	6	—	12.1	
523K+annealed	1.72	273	274	279	153	160	169	17.9	17.6	16.7	[34]
	0.4	280	281	291	158	167	183	20.3	19	18.6	
473K+annealed	1	290	—	—	254	—	—	12.5	—	—	[35]
823K+ annealed	1	245	235	240	146	110	92	20.3	27.2	25.7	[36]
498K+ annealed		264	255	262	190	170	168	21	26.8	24.7	
673K+ annealed	1.2	272	280	283	161	176	182	19.7	18.1	19.6	[17]
		267	263	265	158	159	161	23.2	19.1	20.6	
		255	268	268	122	158	161	23.7	19.1	19.4	

Table 2. Frequency of low angle grain boundaries (LAGBs) and high angle grain boundaries (HAGBs) in the original and as-rolled sheets.

Mis-orientation angles	as-received	pass 1	pass 2	pass 3	pass 4	pass 5
LAGBs($\leqslant 15^{o}$)	72%	33%	28%	20%	31%	30%
HAGBs($>15^{o}$)	28%	67%	72%	80%	69%	70%

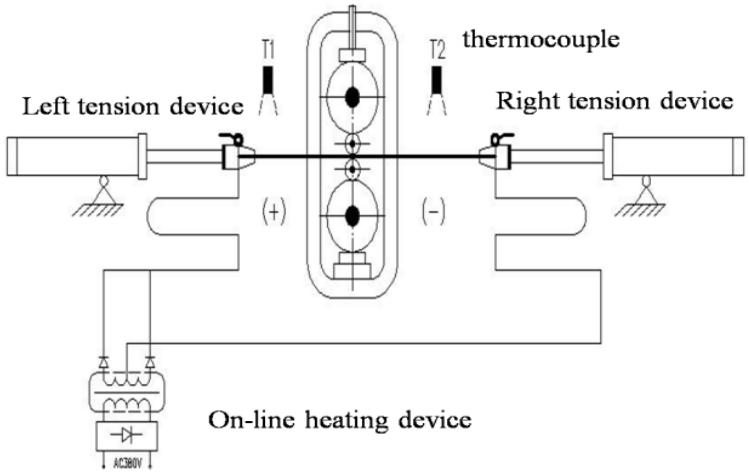

Fig. 1. Schematic drawing of on-line heating rolling [21]. The on-line heating is carried out by electric-resistance heating through the Mg alloy sheet. This allows good control of the temperature of the Mg alloy sheet.

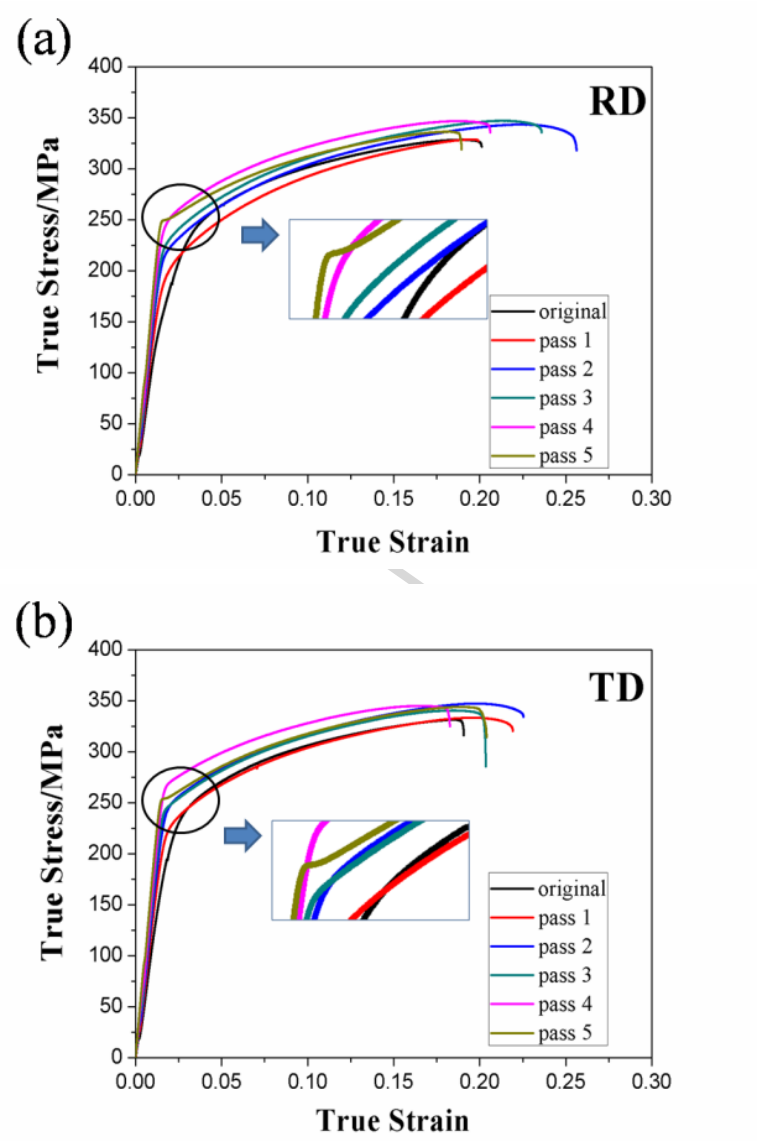

Fig. 2. True stress versus strain curves of as-rolled AZ31B alloy after various roll passes: (a) RD; (b) TD.

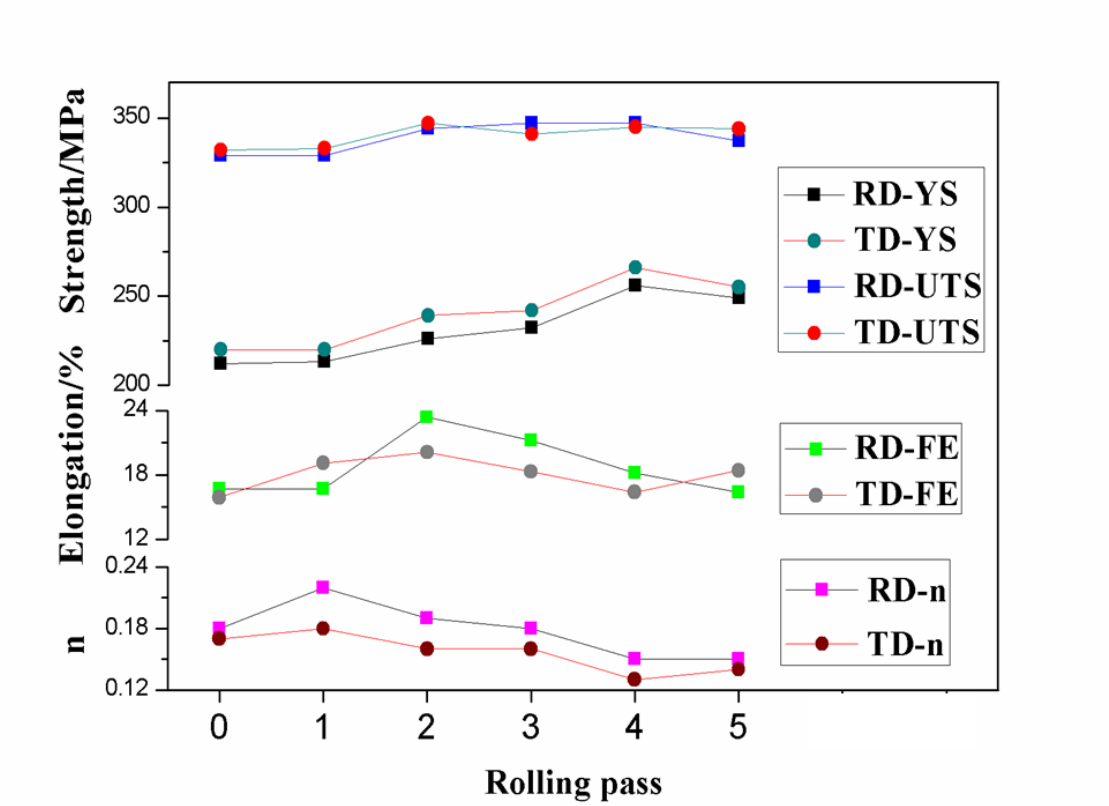

Fig. 3. Mechanical properties of the as-rolled AZ31B alloy thin sheets after various roll passes.

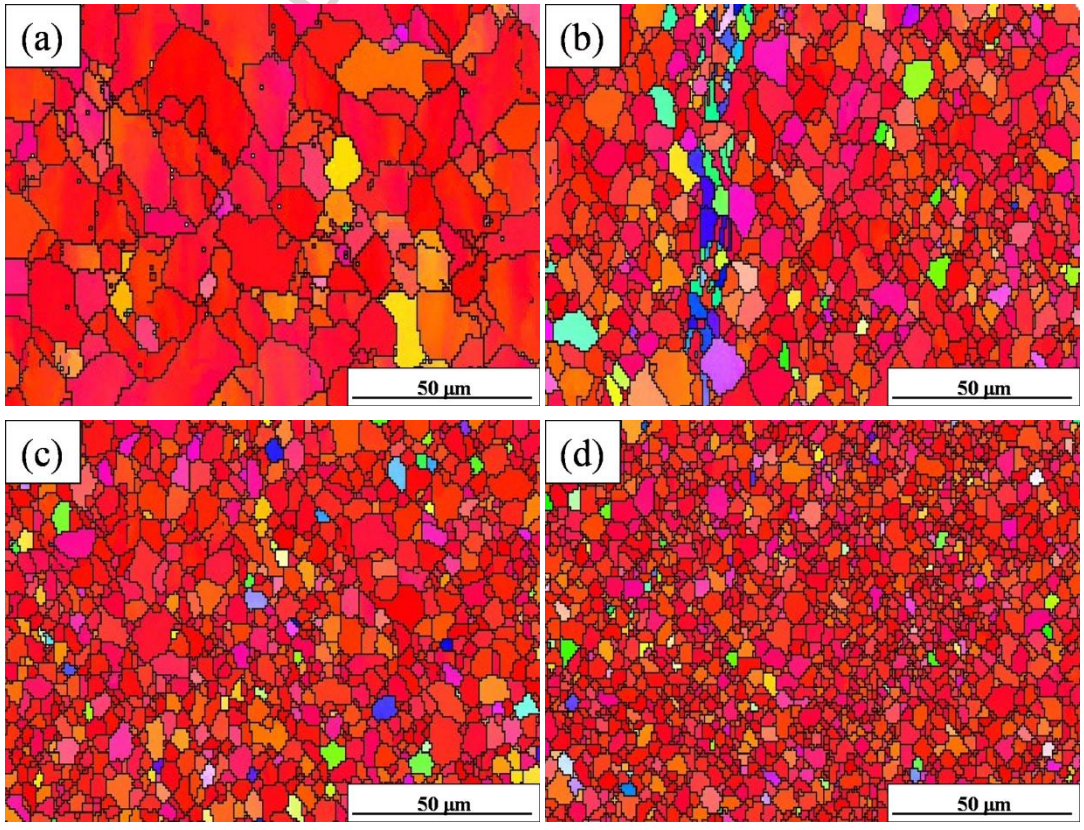

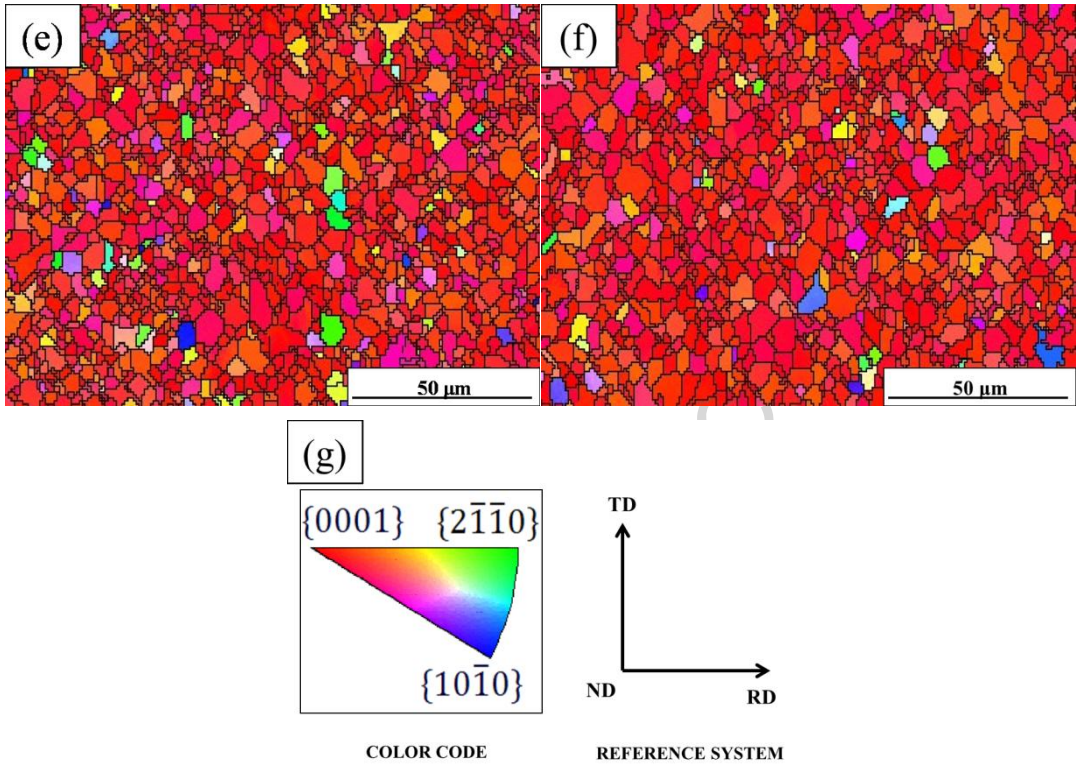

Fig. 4. EBSD inverse pole figure (IPF) maps of the original and as-rolled AZ31B Mg alloy: (a) original[21]; (b) pass 1; (c) pass 2; (d) pass 3; (e) pass 4 ; (f) pass 5 and (g) color code and reference system.

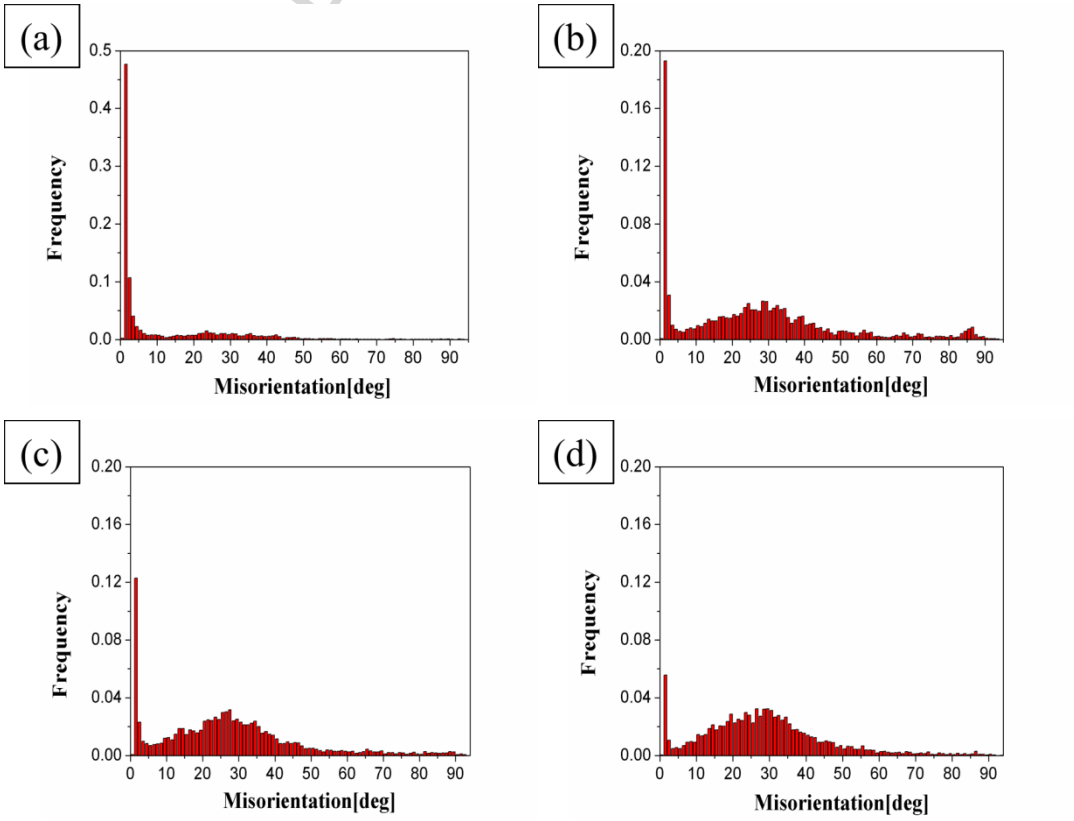

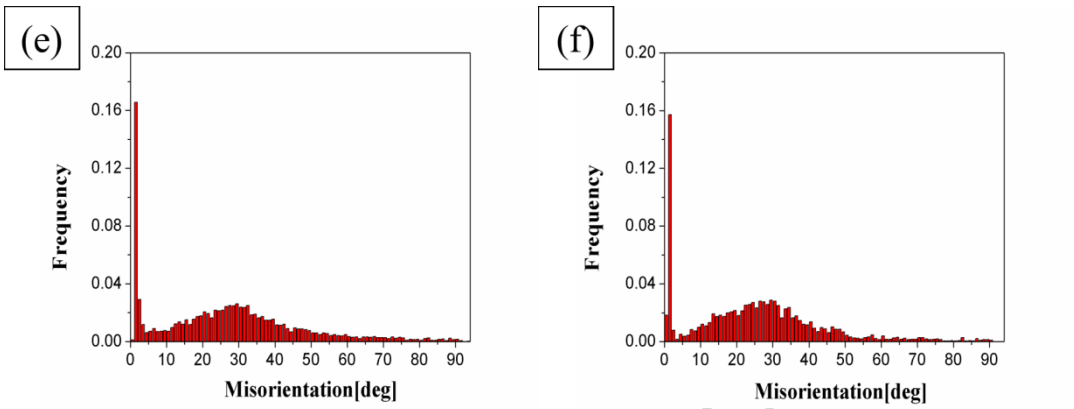

Fig. 5. Frequency-misorientation maps of AZ31B thin sheets rolled at: (a) original; (b) pass 1; (c) pass 2; (d) pass 3; (e) pass 4 and (f) pass 5.

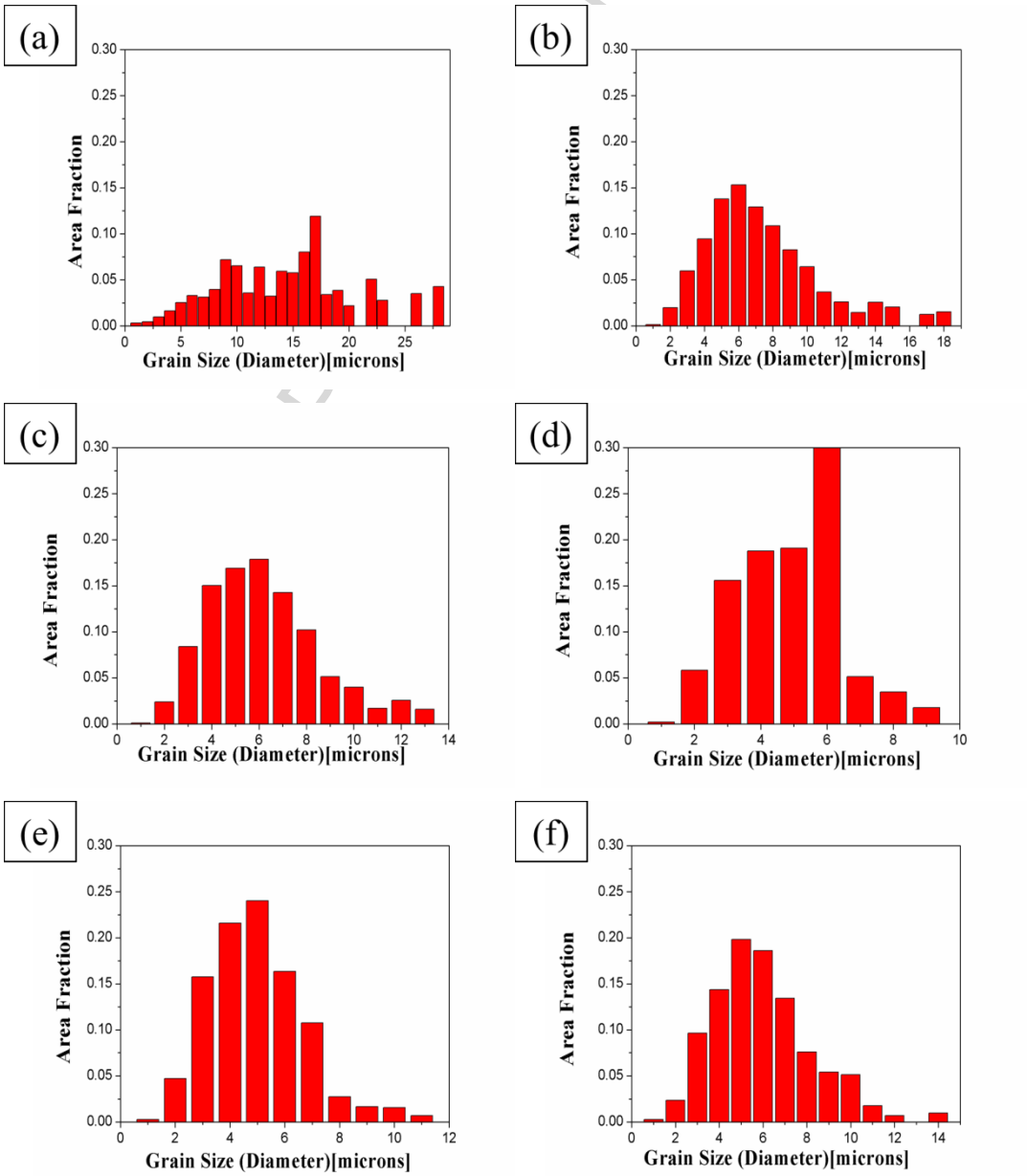

Fig. 6. Grain size distributions of AZ31B thin sheets rolled at: (a) original; (b) pass 1; (c) pass 2; (d) pass 3; (e) pass 4 and (f) pass 5.

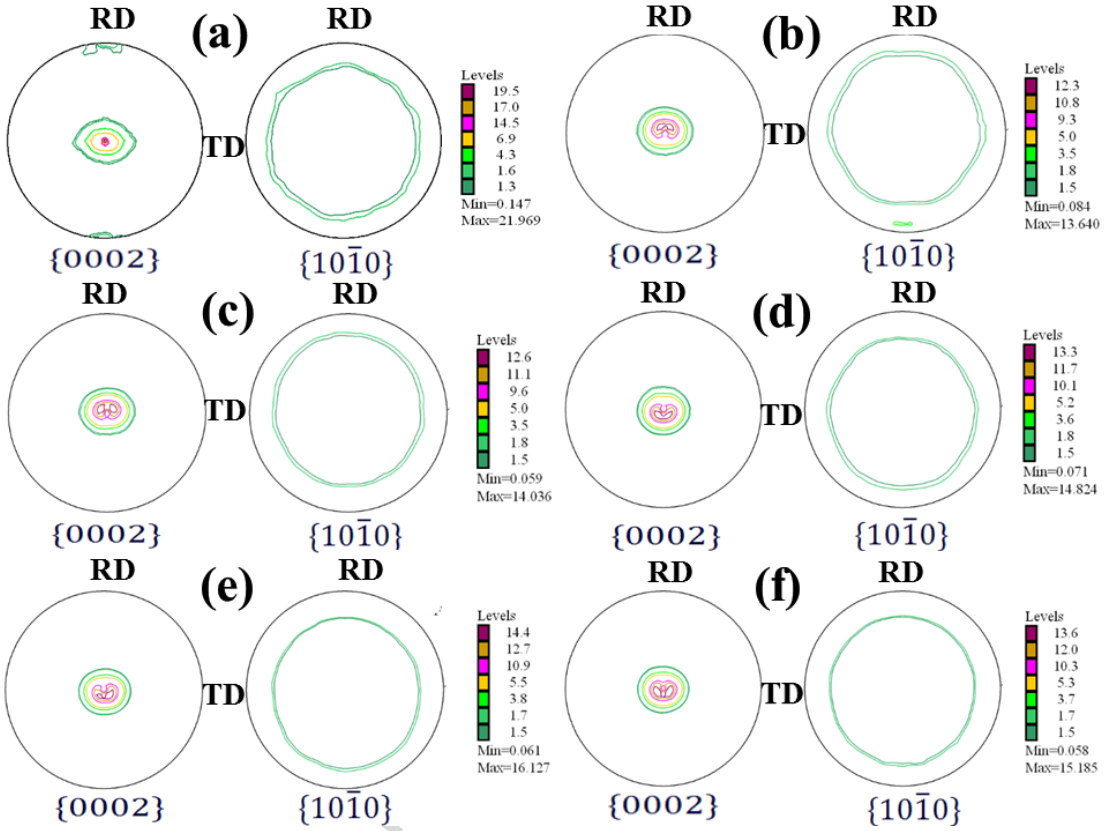

Fig. 7. {0002} and {10$\bar{1}$0}pole figures of AZ31B alloy thin sheets after different rolling passes: (a) original[21]; (b) pass 1; (c) pass 2; (d) pass 3; (e) pass 4 and (f) pass 5.

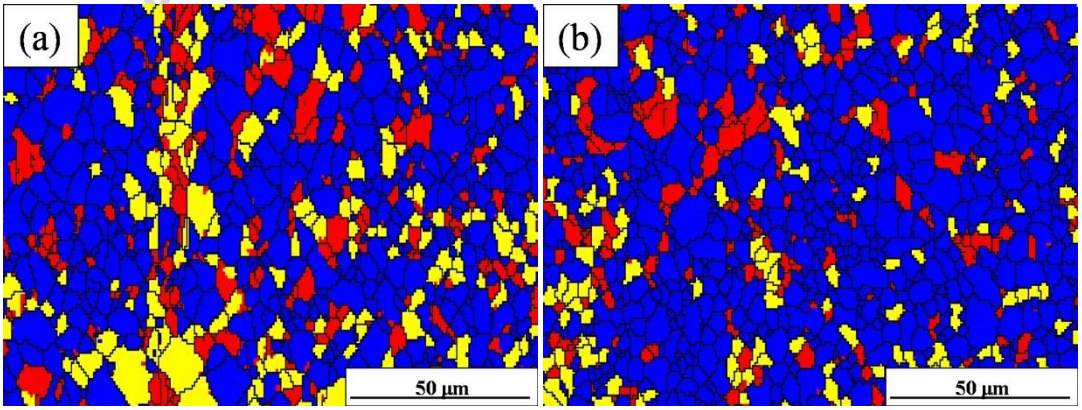

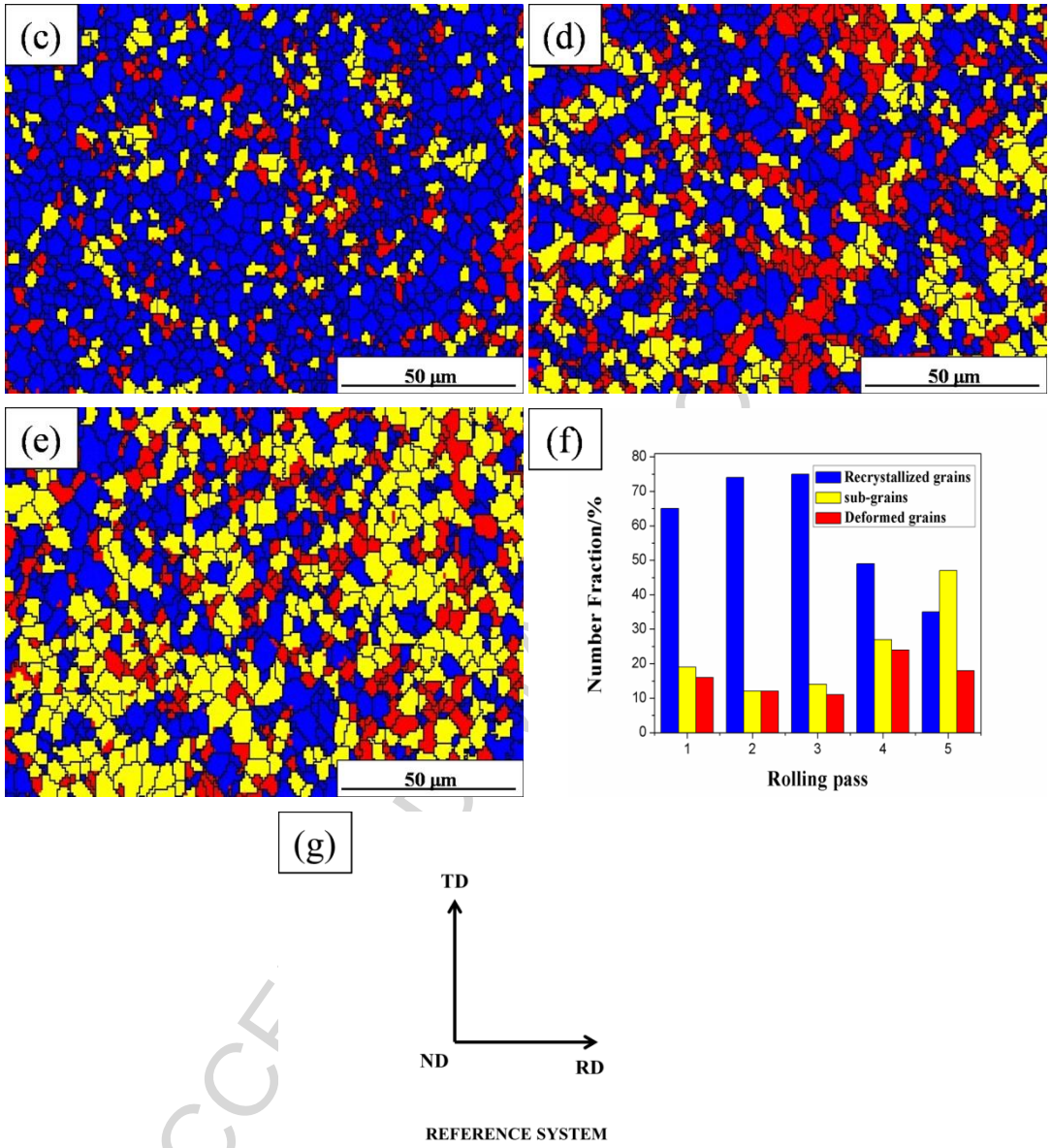

Fig. 8. EBSD maps showing recrystallized regions (blue areas), sub-grains (yellow areas) and deformed regions (red areas): (a) pass 1; (b) pass 2; (c) pass 3; (d) pass 4; (e) pass 5; (f) the distribution proportion of different grain types and (g) reference system.

Highlights:

1. AZ31B sheets were processed by on-line-heating rolling (ON-LHR).

2. The grain size was reduced to 4.1 μm due to dynamic recrystallization.

3. The YS, UTS and fracture elongation reached 232 MPa, 347 MPa and 21%.

4. The rolled sheets had a strong basal texture.

5. The strong texture indicated discontinuous dynamic recrystallization